Proceedings of the 30th International Cosmic Ray Conference ID 777
Rogelio Caballero, Juan Carlos D'Olivo, Gustavo Medina-Tanco,
Lukas Nellen, Federico A. Sánchez, José F. Valdés-Galicia (eds.)
Universidad Nacional Autónoma de México,
Mexico City, Mexico, 2008
Vol. 3 (OG part 2), pages 1237–1240

30TH INTERNATIONAL COSMIC RAY CONFERENCE

Potential Neutrino Signals in a Northern Hemisphere Neutrino Telescope from Galactic Gamma-Ray Sources

A. KAPPES[1,2], C. STEGMANN[3], F. AHARONIAN[4,5] AND J. HINTON[6]
[1]*Physics Dept. University of Wisconsin, Madison WI 53703. USA*
[2]*on leave of absence from Universität Erlangen-Nürnberg, D-91058 Erlangen. Germany*
[3]*Physics Institute, Friedrich-Alexander-University Erlangen-Nuremberg, D-91058 Erlangen. Germany*
[4]*Max-Planck-Institut für Kernphysik, D-69117 Heidelberg. Germany*
[5]*Dublin Institute for Advanced Studies, Dublin 2. Ireland*
[6]*School of Physics and Astronomy, The University of Leeds, Leeds LS2 9JT. UK*
kappes@icecube.wisc.edu

Abstract: Neutrino energy spectra have been calculated based on the recently measured energy spectra of Galactic very high energy γ-ray sources. Based on these neutrino spectra the expected event rates in the ANTARES neutrino telescope and a future km^3 sized neutrino telescope in the Mediterranean Sea, KM3NeT, have been calculated. For the brightest γ-ray sources we find event rates of the order of one neutrino per year in a detector with an instrumented volume of $1\,\mathrm{km}^3$. Although the neutrino event rates are comparable to the background from atmospheric neutrinos the detection of individual sources seems possible.

Introduction

Nearly a century after the discovery of cosmic rays (CR) the origin of this highly energetic hadronic radiation still remains to be a mystery. Compelling evidence for CR accelerators would be the detection of cosmic TeV neutrinos. But still after many years of intense research no high energy cosmic neutrino has been identified yet.

Neutrinos are produced in hadronic interactions of high energy hadrons with the ambient gas in the decay of charged pions and kaons. Neutral pions produced together with charged pions in hadronic interactions decay into photons leading to very high energy (VHE) γ-rays. Thus under the assumption of a hadronic origin VHE γ-rays sources are excellent tracers of potential neutrino sources.

Recently the H.E.S.S. experiment provided a seemingly complete population of bright Galactic VHE γ-ray sources [1]. The majority of the Galactic VHE γ-ray sources are in the southern hemisphere and are thus visible only from a Northern Hemisphere neutrino telescope. We considered the ANTARES detector currently under construction in the Mediterranean Sea, and a planned km^3 scale detector in the Mediterranean Sea, KM3NeT. To derive the expected neutrino event rates we used a new parametrisation of the neutrino spectrum for a given γ-ray spectrum [2], as described in Section 2, together with a full Monte Carlo simulation of the neutrino telescopes, as described in Section 3. This paper summarised the results of this calculation. A more comprehensive discussion of potential Galactic neutrino sources and event rates can be found in [3].

Galactic γ-ray sources

The Galactic VHE γ-ray sources detected by the H.E.S.S. experiment fall into 5 different categories. Each source category originates more or less likely from hadronic interactions.

A) Unambiguously associated with an supernova remnant (SNR) shell: In total 5 SNRs have now been detected and two young shell type SNR, RX J1713.7−3946 and RX J0852.0−4622, are very bright ($\sim 10^{-10}$ erg cm^{-2} s^{-1} for $0.5\,\mathrm{GeV} <$

$E < 10\,\mathrm{GeV}$). Young shell type SNR are the most promising candidates for hadronic acceleration sites. The morphological and spectrometric characteristics of the VHE γ-ray emission from the two bright young SNRs have been studied by H.E.S.S. in great detail. If the VHE γ-ray emission of these sources originates from hadronic interaction the neutrino spectra can be calculated with good accuracy in the most relevant energy band between 0.1 TeV and 100 TeV.

B) Associated with a binary system: This class contains the microquasar LS 5039 and the pulsar PSR B1259−63. The production mechanism of the VHE γ-ray emission is generally believed to be due to inverse Compton scattering of high energy electrons off the ambient photon fields. However, hadronic interpretations of the VHE γ-ray emission from the microquasar LS 5039 exist [4] and cannot be excluded for the pulsar PSR B1259−63.

C) Lacking any good counterpart at other wavelengths: We interpret the lack of any good counterpart at other wavelengths as a indication of a hadronic origin of the VHE γ-ray emission and treat these sources as good candidates for hadronic acceleration sites.

D) Plausibly associated with a pulsar wind nebula (PWN): The VHE γ-ray emission of the objects in this class is generally interpreted in terms of a leptonic (inverse Compton) scenario. But here—as well as in class B)—an hadronic interpretation of the VHE γ-ray emission in terms of hadronic interactions seems possible and exists for Vela X [5].

E) Sources that don't fall in any of the categories mentioned above.

A full listening of the sources taken into account can be found in Table 1. In this paper, neutrino fluxes are calculated for all objects in classes A, B, C and D.

Neutrino fluxes

Starting with a primary proton population with an energy spectrum of

$$\frac{\mathrm{d}N_p}{\mathrm{d}E_p} = k_p \left(\frac{E_p}{1\mathrm{TeV}}\right)^{-\alpha} \exp\left(-\frac{E_p}{\epsilon_p}\right), \quad (1)$$

the γ-ray and neutrinos fluxes from pp-interactions are described by [2]

$$\frac{\mathrm{d}N_{\gamma/\nu}}{\mathrm{d}E_{\gamma/\nu}} \approx k_{\gamma/\nu} \left(\frac{E_{\gamma/\nu}}{1\mathrm{TeV}}\right)^{-\Gamma_{\gamma/\nu}} \exp\left(-\sqrt{\frac{E_{\gamma/\nu}}{\epsilon_{\gamma/\nu}}}\right), \quad (2)$$

with:

$$\begin{aligned} k_\nu &\approx (0.71 - 0.16\alpha)\, k_\gamma, \\ \Gamma_\nu &\approx \Gamma_\gamma \approx \alpha - 0.1, \\ \epsilon_\nu &\approx 0.59\,\epsilon_\gamma \approx \epsilon_p/40. \end{aligned}$$

Equation 2 provides a satisfactory fit to the γ-ray spectra of all sources detected by H.E.S.S. Figure 1 shows as example the γ-ray and resulting neutrino spectra of the SNR RX J1713.7−3946. A power law without cut-off ($\epsilon_\gamma = \infty$) was fitted to the spectra of sources with no published claim of a curvature.

Several assumptions were made in the modelling of the neutrino spectra: no significant contribution of non-hadronic processes to the measured γ-ray signal; no significant γ-ray absorption within the source, i.e. radiation and matter densities are sufficiently low for most of the γ-ray photons to escape; no significant $p\gamma$ interaction (radiation density low); charged pions decay before interacting (matter density is low); muons decay without significant energy loss (magnetic field is low); nucleus-nucleus interactions produce pion spectra which are similar enough to the pp case that they can be treated in the same way; the size of the emitting region within each source is large enough that oscillations will produce a fully mixed neutrino signal at the Earth ($\nu_e : \nu_\mu : \nu_\tau = 1 : 1 : 1$).

Neutrino event rates

Signal event rates: Given a neutrino spectrum $\mathrm{d}N_\nu/\mathrm{d}E_\nu$ from a source the event rate in a neutrino telescope can be calculated as:

$$\frac{\mathrm{d}N_\nu}{\mathrm{d}t} = \int \mathrm{d}E_\nu\, A_\nu^{\mathrm{eff}} \frac{\mathrm{d}N_\nu}{\mathrm{d}E_\nu}\,. \quad (3)$$

Here, A^{eff} is the effective area of the detector comprising the neutrino attenuation in the Earth, the neutrino conversion probability, and the muon detection efficiency of the neutrino telescope. The

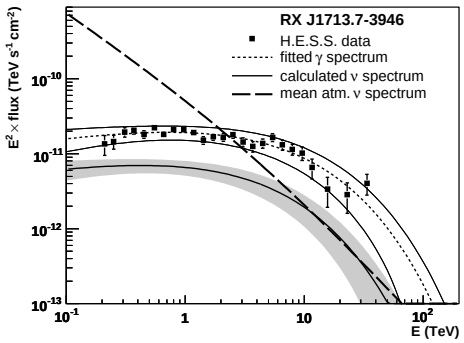

Figure 1: The H.E.S.S. measured γ-ray flux and the estimated neutrino flux together with the atmospheric neutrino flux for the SNR RX J1713−3946. The error bands indicate the $1\,\sigma$ errors including systematic uncertainties from the H.E.S.S. measurements.

effective areas of ANTARES and KM3NeT are displayed in Fig. 2, where for the latter an instrumented volume of $1\,\mathrm{km}^3$ was assumed. Both telescope provide a good visibility on the Galactic VHE γ-ray sources which is taken into account for the actual event numbers after a given observation time. The calculated event numbers for KM3NeT after 5 years of observation are shown in Table 1. The expected event numbers for the ANTARES telescope are about a factor 25 lower.

Background event rates: Neutrinos produced in hadronic interactions of charged cosmic rays on the opposite side of the Earth (atmospheric neutrinos) result in neutrino signals in the telescope indistinguishable from those of cosmic neutrinos. We used the parametrisation of the atmospheric neutrino flux of [6] which reasonable well describes the energy and zenith angle dependence of the atmospheric neutrino flux. The optimal search window is given as $\Theta_{\mathrm{opt}} = 1.6 \times \sqrt{\sigma^2_{\mathrm{PSF}} + \sigma^2_{\mathrm{src}}}$, where σ_{PSF} is the point spread function of the telescope (0.4° for both telescopes) and σ_{src} is the RMS width of the source. The calculated event numbers for atmospheric neutrinos for KM3NeT for 5 years of observation are displayed in Table 1. Again, the event numbers for atmospheric neutrinos for the ANTARES telescope are about a factor 25 lower.

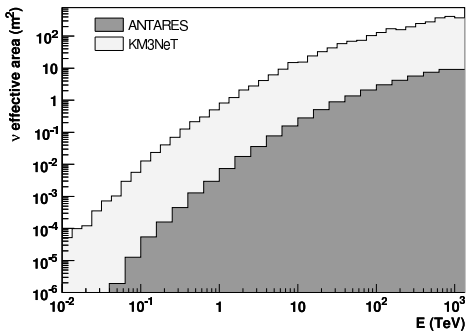

Figure 2: The effective areas of the ANTARES and KM3NeT detectors.

Conclusion

The brightest γ-ray sources produce neutrino rates above 1 TeV comparable to the background from atmospheric neutrinos. The expected event rates of the brightest sources in the ANTARES detector make a detection of cosmic neutrino sources unlikely. However, for a km^3 sized detector event rates of the order of a few neutrinos per year from the brightest sources are expected and the detection of significant signals seems possible.

Acknowledgements

A. Kappes acknowledges the support by the EU Marie-Curie OIF Program.

References

[1] H. sources: see http://www.mpi hd.mpg.de/hfm/hess.
[2] A. Kelner, F. Aharonian, V. Bugayov, Phys. Rev. D 74 (2006) 034018.
[3] A. Kappes, J. Hinton, C. Stegmann, F. Aharonian, Astrophys. J. 656 (2007) 870, (astro-ph/0607286).
[4] F. Aharonian, L. Anchordoqui, D. Khangulyan, T. Montaruli, J. Phys. Conf. Series 39 (2006) 408.
[5] D. Horns, F. Aharonian, A. Santangelo, A. Hoffmann, C. Masterson, A&A 451 (2006) L51.
[6] L. Volkova, Sov. J. Phys. 31(6) (1980) 784.

Table 1: H.E.S.S. catalogue sources [1] with range of estimated neutrino event rates within the search window in KM3NeT ($1\,\mathrm{km}^3$ instrumented volume) for 5 years of operation together with the expected atmospheric neutrino background for neutrino energies above 1 TeV and 5 TeV. The column *Dia* displays the diameter of the source and the column *Vis.* shows the visibility (fraction of time when the source is below the horizon) of the source to KM3NeT. The spectra of all sources marked with an asterisk are fitted to a power law without exponential cut-off.

				$E > 1\,\mathrm{TeV}$		$E > 5\,\mathrm{TeV}$	
Source name		Dia (°)	Vis	N_{src}	N_{atm}	N_{src}	N_{atm}
Source class A (supernova remnants)							
RX J0852.0−4622		2.0	0.83	11	104	4.2	21
RX J1713.7−3946		1.3	0.74	11	41	4.6	8.2
HESS J1640−465	*	0.1	0.83	2.2	8.7	1.3	1.8
HESS J1745−290 †	*	< 0.1	0.65	2.0	6.4	1.3	1.3
HESS J1834−087	*	0.2	0.54	1.1	6.0	0.7	1.2
HESS J1713−381	*	0.1	0.73	0.6	7.2	0.4	1.4
Source class B (binary systems)							
LS 5039 (INFC) ††		0.1	0.57	0.5	2.5	0.2	0.5
LS 5039 (SUPC) ††	*	0.1	0.57	0.2	3.0	0.1	0.6
PSR B1259−63	*	< 0.1	1.00	0.6	9.1	0.3	1.7
Source class C (no counterparts at other wavelengths)							
HESS J1303−631		0.3	1.00	1.6	11	0.3	2.1
HESS J1745−303	*	0.4	0.66	9	9.0	7	1.8
HESS J1614−518	*	0.5	1.00	6	19	3.7	4.0
HESS J1837−069	*	0.2	0.53	3.3	5.9	2.2	1.2
HESS J1634−472	*	0.2	0.85	1.7	9.8	1.1	2.0
HESS J1708−410	*	0.1	0.76	1.1	7.6	0.7	1.5
Source class D (pulsar wind nebula)							
Vela X		0.8	0.81	16	23	10	4.6
HESS J1825−137		0.5	0.57	8	9.3	3.7	1.8
Crab Nebula		< 0.1	0.39	5.8	5.2	1.9	1.1
HESS J1632−478	*	0.3	0.87	9	12	7	2.4
MSH 15−52	*	0.2	1.00	7.1	10	4.7	2.0
HESS J1616−508	*	0.3	1.00	6.6	14	4.1	3.0
HESS J1420−607	*	0.1	1.00	4.6	9.6	3.1	1.9
HESS J1418−609	*	0.1	1.00	4.2	9.6	3.0	1.9
HESS J1809−193	*	0.4	0.59	3.7	8.2	2.6	1.6
HESS J1813−178	*	0.1	0.59	3.2	5.8	2.4	1.1
HESS J1702−420	*	0.2	0.77	2.1	8.4	1.4	1.7
HESS J1804−216	*	0.4	0.61	1.5	8.4	0.7	1.7
HESS J1718−385	*	0.1	0.73	1.1	7.3	0.8	1.5
G 0.9+0.1	*	< 0.1	0.65	0.6	6.2	0.4	1.2
Source class E (other)							
HESS J1023−575	*	0.3	1.00	3.1	13	1.7	2.5

† Source association is uncertain; might be associated to the SNR Sagitarius A East or to the Galactic Centre black hole Sagitarius A*.

†† Assuming no γ-ray absorption within the source. INFC and SUPC specify the two phases of inferior and superior conjunction of the binary system.